Published in final edited form as:

Cell Rep. 2019 September 03; 28(10): 2517–2526.e5. doi:10.1016/j.celrep.2019.08.006.

Proteomic Analysis Identifies Membrane Proteins Dependent on the ER Membrane Protein Complex

Songhai Tian[1,6], **Quan Wu**[1,2,6], **Bo Zhou**[3], **Mei Yuk Choi**[4], **Bo Ding**[5], **Wei Yang**[3], **Min Dong**[1,7,*]

[1]Department of Urology, Boston Children's Hospital, and Department of Surgery and Department of Microbiology, Harvard Medical School, Boston, MA 02115, USA

[2]Central Laboratory of Medical Research Centre, The First Affiliated Hospital of USTC, Division of Life Sciences and Medicine, University of Science and Technology of China, Hefei, Anhui 230001, People's Republic of China

[3]Division of Cancer Biology and Therapeutics, Departments of Surgery and Biomedical Sciences, Samuel Oschin Comprehensive Cancer Institute, Cedars-Sinai Medical Center, Los Angeles, CA 90048, USA

[4]Division of Genetics, Brigham and Women's Hospital, and Harvard Medical School, Boston, MA 02115, USA

[5]Bonacept LLC, San Diego, CA 92122, USA

[6]These authors contributed equally

[7]Lead Contact

SUMMARY

The endoplasmic reticulum (ER) membrane protein complex (EMC) is a key contributor to biogenesis and membrane integration of transmembrane proteins, but our understanding of its mechanisms and the range of EMC-dependent proteins remains incomplete. Here, we carried out an unbiased mass spectrometry (MS)-based quantitative proteomic analysis comparing membrane proteins in EMC-deficient cells to wild-type (WT) cells and identified 36 EMC-dependent membrane proteins and 171 EMC-independent membrane proteins. Of these, six EMC-dependent and six EMC-independent proteins were further independently validated. We found that a common feature among EMC-dependent proteins is that they contain transmembrane domains (TMDs) with polar and/or charged residues. Mutagenesis studies demonstrate that EMC dependency can be

*Correspondence: min.dong@childrens.harvard.edu.

AUTHOR CONTRIBUTIONS

S.T. and M.D. initiated the project and designed the experiments. S.T. carried out the majority of the experiments and was assisted by Q.W. B.Z. and W.Y. carried out mass spectrometry and statistical analyses. M.Y.C. assisted with genotyping. B.D. assisted with the bioinformatic analysis. S.T. and M.D. wrote the manuscript with input from all co-authors.

DECLARATION OF INTERESTS

The authors declare no conflicts of interest.

SUPPLEMENTAL INFORMATION

Supplemental Information can be found online at https://doi.org/10.1016/j.celrep.2019.08.006.

converted in cells by removing or introducing polar and/or charged residues within TMDs. Our studies expand the list of validated EMC-dependent and EMC-independent proteins and suggest that the EMC is involved in handling TMDs with residues challenging for membrane integration.

In Brief

The endoplasmic reticulum membrane protein complex (EMC) contributes to the biogenesis of transmembrane proteins. Using mass spectrometry-based quantitative proteomic analysis, Tian et al. identify EMC-dependent and EMC-independent proteins. The authors find evidence that the EMC is involved in handling transmembrane domains with polar and/or charged residues that are challenging for membrane integration.

Graphical Abstract

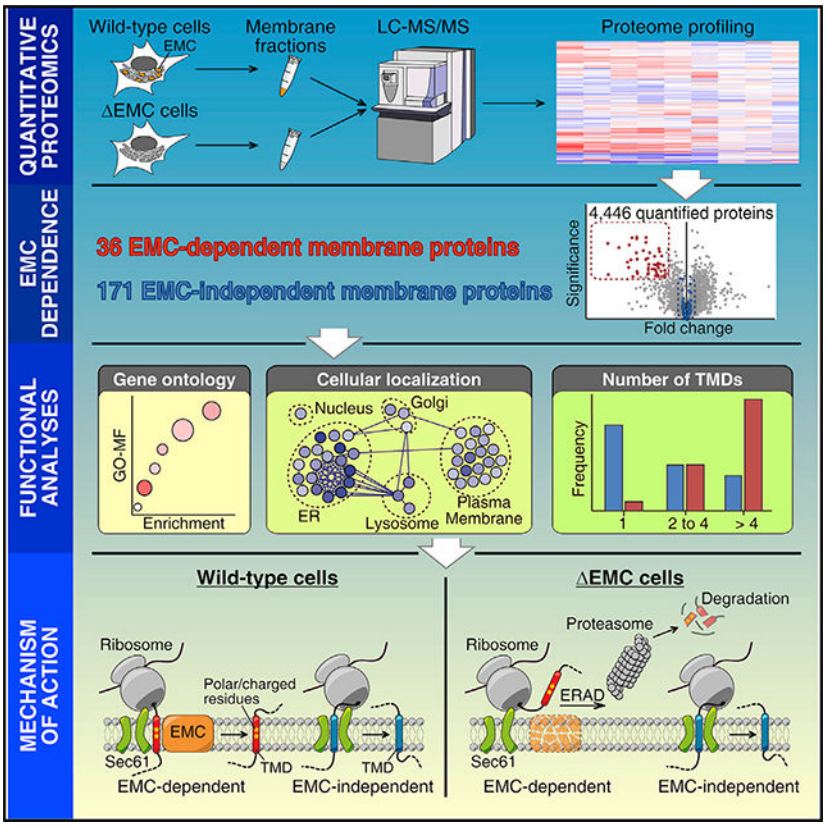

INTRODUCTION

The endoplasmic reticulum (ER) is the site for biosynthesis and membrane integration of transmembrane proteins in eukaryotic cells, primarily mediated by the Sec61 translocon through signal recognition particle (SRP)-dependent co-translational insertion (Rapoport et al., 2017). Additional mechanisms mediate membrane insertion of tail-anchored (TA) proteins post-translationally, such as the transmembrane domain (TMD) recognition complex (TRC) and the guided entry of TA proteins (GET) pathway (Denic et al., 2013;

Hegde and Keenan, 2011; Shao and Hegde, 2011). Many additional chaperones are involved to ensure correct membrane insertion and folding of diverse TMDs (Rapoport et al., 2017).

The multi-subunit ER membrane protein complex (EMC) was recently shown to contribute to proper biosynthesis and/or membrane insertion of transmembrane proteins on the ER (Chitwood and Hegde, 2019). It was initially identified in yeast, with six subunits (EMC1–EMC6) (Jonikas et al., 2009). The EMC is highly conserved across eukaryotic species, except for a few single-cell organisms (Wideman, 2015). Mammals contain 10 EMC members. EMC1, EMC3, EMC4, EMC5, EMC6, EMC7, and EMC10 contain TMDs, while EMC2, EMC8, and EMC9 are cytosolic proteins. Yeast protein Sop4 and YDR056C were recognized as homologs of EMC7 and EMC10, respectively (Wideman, 2015). The mammalian EMC was initially identified as one of the interactors with ER-associated protein degradation (ERAD) components (Christianson et al., 2011). Loss of EMC members reduces the expression of many different transmembrane proteins, including Yor1 in yeast (Louie et al., 2012); acetylcholine receptors (AChRs) and gamma-aminobutyric acid (GABA) receptors in *C. elegans* (Richard et al., 2013); rhodopsin, the alpha subunit of Na^+K^+-ATPase, transient receptor potential channel (TRP) in *D. melanogaster* (Satoh et al., 2015); a member of ATP-binding cassette (ABC) transporters (ABCA3) in mice (Tang et al., 2017); sterol-*O*-acyltransferase 1 (SOAT1) and squalene synthase (SQS, also known as FDFT1) in mammalian cells (Volkmar et al., 2019); and the mutant forms of cystic fibrosis transmembrane conductance regulator (CFTR) and connexin 32 that are associated with human diseases (Coelho et al., 2019; Louie et al., 2012). It has been shown that a loss of EMC members destabilizes these membrane proteins during their biosynthesis and leads to their degradation (Richard et al., 2013; Satoh et al., 2015; Shurtleff et al., 2018).

A loss or reduction of EMC members has been shown to be associated with irregularity in many cellular processes (Bagchi et al., 2016; Harel et al., 2016; Lahiri et al., 2014; Li et al., 2013; Shen et al., 2016; Volkmar et al., 2019). It is possible that these defects are secondary to the loss of certain key membrane proteins. Multiple members of the EMC have been identified as host factors in genome-wide screens for flaviviruses, including yellow fever, Zika, West Nile, Dengue, and Japanese encephalitic virus (Ma et al., 2015; Marceau et al., 2016; Savidis et al., 2016; Tao et al., 2016; Zhang et al., 2016), and it has been shown that the EMC is required for biosynthesis of viral non-structural multi-pass transmembrane proteins (Lin et al., 2019). EMC members have also been identified in a genome-wide screen for host factors of the bacterial toxin *C. difficile* toxin B (TcdB), as the loss of EMC members reduces the expression of the 7-pass membrane Wnt receptor Frizzled (FZD) 1, 2, and 7, which are receptors of TcdB (Tao et al., 2016).

Recent studies demonstrated that the EMC acts as an insertase for membrane insertion of TA proteins containing TMDs with low levels of hydrophobicity (Guna et al., 2018). It was also shown that the EMC is required for the accurate insertion of the first TMD of a subset of G-protein-coupled receptors (GPCRs) (Chitwood et al., 2018). Consistent with the idea that the EMC acts as an insertase, EMC3 is a distant homolog of Get1, which is a part of the insertase for handling TA proteins, and both EMC3 and Get1 are linked to the prokaryotic insertase YidC (Anghel et al., 2017).

The EMC was also shown to interact with many multi-pass membrane proteins co-translationally and promote their biosynthesis (Shurtleff et al., 2018). Proteomic studies using the stable isotope labeling with amino acids in cell culture (SILAC) technique and quantitative mass spectrometry (MS) analysis of EMC2 and EMC4 knockdown cells (via CRISPRi) identified a list of potential EMC client proteins (Shurtleff et al., 2018).

Here, we generated EMC4- and EMC6-deficient cells and carried out unbiased MS-based quantitative proteomic analysis to compare the expression of membrane proteins in EMC-deficient and wild-type (WT) cells. A number of EMC-dependent and EMC-independent transmembrane proteins were identified and validated. Mutagenesis studies further demonstrated that EMC dependency can be converted by removing or introducing polar and/or charged residues within TMDs.

RESULTS

EMC4- and EMC6-Deficient Cells

Among the 10 EMC members (Figure S1A), EMC4 and EMC6 are the highest-ranking hits identified in our previous genetic screens for TcdB (Tao et al., 2016). To understand the role of the EMC, we generated EMC4- and EMC6-deficient HeLa cells using the CRISPR-Cas9 approach (Figures S1A–S1C). Three EMC4-deficient, three EMC6-deficient, and four WT single-cell clones were isolated and established.

HeLa cells contain three sets of chromosomes, and the genotypes of each clone were determined through sub-clonal sequencing (Figures 1A, S1B, and S1C). The three EMC4-deficient cell clones are designated EMC4-Mut. EMC4-Mut-3 contains two alleles with frameshift mutations and one allele with a 12 base-pair (bp) deletion. EMC4-Mut-6 has one allele with a frameshift mutation and two alleles with a 12-bp deletion. EMC4-Mut-10 has one frameshift allele, one allele with a 12-bp deletion, and one allele with a 3-bp deletion. All three EMC6-deficient cell clones contain frameshift mutations on all three alleles (designated EMC6-KO-4, EMC6-KO-6, and EMC6-KO-20). These EMC4-Mut and EMC6-KO cells appear to be normal with no obvious growth defects.

To further confirm that these cells are deficient in EMC4 or EMC6, we compared their sensitivity to a truncated version of TcdB ($TcdB_{1–1830}$) versus WT cells (Tao et al., 2016). All six EMC4- and EMC6-deficient cell lines are several-fold less sensitive to $TcdB_{1–1830}$ compared with WT cells (WT-1, WT-5, WT-8, and WT-13; Figures S1D and S1E).

Quantitative Proteomics Analysis of EMC4- and EMC6-Deficient Cells

We next applied a tandem mass tag (TMT) labeling-based multiplexed quantitative proteomics approach to compare membrane protein levels from the three EMC4-Mut, three EMC6-KO, and three WT clones (WT-1, WT-5, and WT-8; Figure 1B). Cells were harvested and sonicated to isolate the membrane fraction, which was then subjected to trypsin digestion and labeling with 9-plex amino-reactive TMT reagents. The TMT-labeled peptides were mixed and analyzed by two-dimensional (high-pH and low-pH) reversed-phase liquid chromatography tandem MS (LC-MS/MS; Figures 1B and S2A).

In total, 5,570 proteins were identified, of which 4,446 proteins with at least two quantified peptides were selected for statistical analysis (Figure 1C; Data S1). Based on the Gene Ontology Cellular Component (GO-CC) database, 3,188 out of these 4,446 proteins are membrane-associated proteins. Based on a UniProt database search, 971 proteins have the "Transmembrane" feature key.

Heat-map and clustering analyses of all nine samples were carried out for all 4,446 quantified proteins (Figure 1D). As expected, three WT clones and three EMC6-KO clones form two distinct clusters based on Pearson distance clustering analysis. While EMC4-Mut-3 and EMC4-Mut-6 form a cluster close to the EMC6 cluster, EMC4-Mut-10 falls into the WT cluster, suggesting that a single-residue deletion in EMC4-Mut-10 cells may not completely disrupt EMC4 function.

EMC-Dependent Proteins

As EMC4-Mut cells may still retain some levels of EMC4 function, we focused on comparing the expression levels of membrane proteins between the three EMC6-KO cells and the three WT cells. Each of the 4,446 quantified proteins was plotted by its fold changes ($\log_2$ ratios of EMC6/WT) as the x axis and statistical significance (p values of two-tailed Student's t test) as the y axis (Figure 1E). A total of 81 proteins were considered significantly changed ($p < 0.01$): 17 upregulated ($\log_2$ ratio > 0.5) and 64 downregulated ($\log_2$ ratio < -0.5) (Figure S2B).

The most significantly changed proteins are other EMC members (Figure 1E). These results were consistent with previous reports that a loss of individual EMC members leads to reductions of other EMC members (Jonikas et al., 2009; Shurtleff et al., 2018; Volkmar et al., 2019). Besides the seven EMC members, there are 36 downregulated membrane proteins (Data S1). Among them, 13 were identified as significantly downregulated in the previous proteomic analysis of EMC2 and EMC4 knockdown cell lines (Shurtleff et al., 2018), thereby providing a degree of validation (Figure 1F).

Gene Ontology analysis and the enriched Molecular Function (GO-MF) annotations revealed that the 36 EMC clients are denoted as having transmembrane transporter activities (Figure S2C), which is consistent with the previous analysis (Shurtleff et al., 2018). These 36 proteins are distributed across different membranes in cells, including the nuclear envelope, ER, Golgi apparatus, endosome and/or lysosome, and plasma membranes (Figure S2D).

We then plotted all 971 membrane proteins by their number of TMDs (Figure 2A). Among the 36 EMC-dependent proteins, two (ZFPL1 and SGPL1) are single-TMD proteins. ZFPL1 is a TA protein, but SGPL1 is not. The rest of the 34 EMC-dependent proteins contain various numbers of TMDs (Figures 2A). We also selected 171 EMC-independent membrane proteins based on two criteria: (1) the coefficient of variation of the three WT cells and three EMC6 KO cells is less than 10%, and (2) the $\log_2$ ratios of EMC6/WT are between −0.1 and 0.1 (Data S1). These proteins were analyzed for their TMD numbers, and the results showed clearly that EMC-independent proteins can contain any number of TMDs (Figure 2B). These findings demonstrate that EMC dependency is not determined by the number of TMDs.

We further clustered the 36 EMC-dependent, 171 EMC-independent, and 971 identified transmembrane proteins into three groups: single, 2–4, and more than 4 TMDs. Compared with the 171 EMC-independent and all 971 transmembrane proteins, EMC-dependent proteins are enriched within the category of more than 4 TMDs (Figure 2B, insert), suggesting that multi-TMD proteins have a greater likelihood of becoming EMC dependent.

Validation of EMC-Dependent and EMC-Independent Proteins

To validate a subset of EMC-dependent and EMC-independent proteins experimentally, we selected FDFT1 (also known as SQS, 2 TMDs, which has been previously confirmed as an EMC client), CD9 (CD9 antigen, 4 TMDs), ATP6V0A1 (V-type proton ATPase 116 kDa subunit A isoform 1, 8 TMDs), ZFPL1 (zinc finger protein-like 1, 1 TMD, TA), FZD6 (Frizzled-6, 7 TMDs), and SLC43A3 (solute carrier family 43 member 3, 12 TMDs) from the list of 36 EMC-dependent proteins. We also selected SEC61A1 (protein transport protein Sec61 subunit alpha isoform 1, 10 TMDs), ERGIC3 (endoplasmic reticulum-Golgi intermediate compartment protein 3, 2 TMDs), ABCD1 (ATP-binding cassette sub-family D member 1, 5 TMDs), ABCB7 (ATP-binding cassette sub-family B member 7, 6 TMDs), SLC27A4 (long-chain fatty acid transport protein 4, 2 TMDs), and STT3A (Dolichyl-diphospho-oligosaccharide-protein glycosyltransferase subunit STT3A, 11 TMDs) from the list of EMC-independent membrane proteins.

We first screened available antibodies and found that endogenous EMC-dependent proteins FDFT1, CD9, and ATP6V0A1, and EMC-independent protein SEC61A1, can be detected in HeLa cell lysates using their specific antibodies. Consistent with the proteomic analysis, expression of FDFT1, CD9, and ATP6V0A1 are all drastically reduced in EMC4-Mut and EMC6-KO cells compared with WT cells (representative blots shown in Figure 2C and quantification shown in Figure S5), while SEC61A1 showed similar levels of expression across EMC4-Mut, EMC6-KO, and WT cells (Figures 2D and S5Q).

Other selected proteins were fused with different detection tags (FLAG, HA, or 1D4) and expressed via transient transfection in WT, EMC4-Mut, and EMC6-KO cell lines. Expressions of ATP6V0A1, ZFPL1, FZD6, and SLC43A3 are all at much lower levels in EMC4-Mut and EMC6-KO cells compared with WT cells (Figures 2C and S5). On the other hand, ERGIC3, ABCD1, ABCB7, SLC27A4, and STT3A in EMC4-Mut and EMC6-KO cells are expressed at levels similar to those in WT cells (Figures 2D and S5). Blocking proteasome degradation pathways (with MG-132 or Lactacystin) elevated levels of EMC-dependent proteins FDFT1, FZD6, ATP6V0A1, and SLC43A3 in EMC6-KO cells (Figures S3A and S3B), suggesting that EMC-deficiency leads to degradation of these EMC-dependent proteins.

In addition to the 36 identified EMC-dependent proteins, we also examined the expression of FZD1, FZD2, and FZD7 (Tao et al., 2016). FZD1, FZD2, and FZD7 were not detected in MS-based proteomic analysis, likely because these morphogen receptors are expressed at low levels. FZD1, FZD2, and FZD7, tagged with 1D4, all showed much lower expressions in EMC4-Mut and EMC6-KO cells compared with WT cells (Figures S3C–S3J). Importantly, the expression of FZD7 in EMC4-Mut cells can be restored when EMC4 is expressed in EMC4-Mut cells via transient transfection (Figures S3G and S3H). Similarly,

transient transfection of EMC6 in EMC6-KO cells also restored expression levels of FZD7 (Figures S3I and S3J).

Overexpression of EMC-Dependent Proteins Causes UPRs in EMC-Deficient Cells

It has been shown that EMC deficiency induces unfolded protein responses (UPRs; also known as ER stress) in *D. melanogaster* and *C. elegans* (Richard et al., 2013; Satoh et al., 2015), including upregulation of ER chaperones and related proteins such as binding immunoglobulin protein (Bip). To probe whether the UPR pathway is activated in our EMC-deficient cell lines, we compared the expression levels of Bip when EMC-dependent and EMC-independent proteins were overexpressed in EMC-deficient cells via transient transfection. FZD4 is a member of the FZD family and is EMC dependent (Figures S4A and S4B). Synaptotagmin 1 (SYT1) is a type I transmembrane protein with a single TMD. It is expressed in EMC4-Mut cells at similar levels as in WT cells, indicating that it is EMC independent (Figures S4A and S4B). Transfecting EMC4-Mut cells, but not WT cells, with FZD4 or FZD7 increased Bip expression levels, while transfecting SYT1 did not alter Bip levels compared with controls (Figures S4C and S4D), thus confirming that the UPR pathway is induced when EMC-dependent proteins are overexpressed in EMC-deficient cells.

EMC Dependency Is Related to Polar and/or Charged Residues in TMDs

Both our studies and the previous proteomic studies revealed that many EMC clients are classified as transporters, which often contain TMDs with charged or polar residues that are not favorable for membrane insertion. EMCs may thus act as chaperones to facilitate the correct insertion of TMDs that are challenging to handle due to the presence of charged, polar, or other less-hydrophobic residues. These TMDs can be located at any position of a transmembrane protein.

To test this hypothesis experimentally, we carried out mutagenesis studies focusing on altering the residues within TMDs. FDFT1 is predicted to contain two TMDs. It has been shown in *in vitro* reconstitution assays that mutating four polar amino acid residues in the C-terminal TMD of FDFT1 (S397L, Q399L, T402L, and T403L; Figure 3A) converts that TMD of FDFT1 to become EMC independent for membrane insertion (Guna et al., 2018). We introduced the same set of mutations to full-length FDFT1 and examined this mutant form (FDFT1-Mut1) in cells by transient transfection. It showed levels of expression similar to WT FDFT1 in WT cells, indicating that these point mutations do not affect protein expression and/or stability (Figure 3B). While WT FDFT1 expression in EMC4-Mut and EMC6-KO cells is largely diminished, FDFT1-Mut1 was expressed at similar levels across EMC4-Mut, EMC6-KO, and WT cells (Figures 3C and S5). Thus, the mutant FDFT1 becomes EMC independent once the polar residues within its TMD are replaced with hydrophobic ones. Interestingly, WT FDFT1 fused with a 3xFLAG tag (plus a linker, 32 residues in total) at its C terminus also showed similar expression levels across EMC4-Mut, EMC6-KO, and WT cells (Figures S4E and S4F), suggesting that the distance between this TMD and the C terminus also contributes to whether the EMC is involved.

We next tested ZFPL1, which contains a single TMD at the C terminus. Its TMD is fairly hydrophobic but contains a polar residue S284 and a charged residue R285. WT ZFPL1 is dependent on the EMC (Figure 2C). We generated mutant forms of ZFPL1 containing S to L, R to L, as well as the double mutation of both S and R residues (Figure 3D). None of these three mutant forms affects protein expression when expressed in WT cells (Figure 3E). All three mutant forms become EMC independent (Figures 3F and S5).

We then examined CD9, which has 4 TMDs (Figure 3G). Its second TMD has the lowest hydrophobicity among the four. We generated a series of mutations aiming to reduce the presence of polar residues and increase the overall hydrophobicity levels of this TMD. Many mutations affected protein folding/stability and thus were not further studied. We eventually identified a double mutation (T58V/G59A), which creates a mutant CD9 expressed at levels similar to WT CD9 in WT cells (Figure 3H). Thus, this double-mutant form does not affect protein expression and/or stability, but it becomes EMC independent (Figures 3I and S5). Interestingly, neither T58V nor G59A alone is sufficient to convert the dependency on the EMC (Figure 3I).

Mutagenesis Studies of EMC-Independent Proteins

To carry out mutagenesis studies of EMC-independent proteins, we first selected ERGIC3, which contains two TMDs. A series of mutations were explored to change the hydrophobic residues within its second TMD, which has lower hydrophobicity than the other TMD. The expression of these mutants in WT cells was first compared with WT ERGIC3, and mutations that disrupt protein expression and/or stability were not further pursued. One set of mutations, replacing F344Y/L345N (Figure 4A), was expressed at levels similar to WT ERGIC3 in WT cells (Figure 4B), and it maintained the same membrane topology (Figure S4G). This mutant form was expressed at much lower levels in EMC4-Mut and EMC6-KO cells compared with WT cells, indicating that it becomes dependent on the EMC (Figures 4C and S5). Furthermore, expression of this mutant ERGIC3 can be restored by co-transfection of EMC4 in EMC4-Mut cells or EMC6 in EMC6-KO cells (Figures 4D and S5).

We also tested SEC61A1, which has 10 TMDs. We focused on mutations within the second and fifth TMDs, which have low levels of hydrophobicity among the 10 TMDs. Of the mutations tested, we found that replacing three residues (L89N, I90T, and M91Q; Figure 4E) within the second TMD does not affect expression levels of SEC61A1 in WT cells (Figure 4F), but the expression of this mutant is greatly reduced in EMC4-Mut and EMC6-KO cells (Figures 4G and S5). Expression of this mutant SEC61A1 (SEC61A1-FLAG-N-Mut1) in EMC4-Mut cells or EMC6-KO cells was restored by co-transfection with EMC4 or EMC6, respectively (Figures 4H and S5). Thus, introducing these polar residues into the second TMD converted SEC61A1 to become EMC dependent.

DISCUSSION

Here, we carried out unbiased quantitative proteomic analysis comparing expression levels of membrane proteins in EMC-deficient cells versus WT cells. Compared to a recently published proteomic study of EMC-deficient cells (Shurtleff et al., 2018), the majority of the identified proteins (3,920) were shared between the two studies. Utilizing stringent criteria,

we selected a list of 171 transmembrane proteins as EMC independent and 36 as EMC dependent. Of the 36 EMC-dependent proteins, 23 were uniquely identified in this study, including seven (ALG10, SLC9A7, SLC44A2, CLCN3, TMEM19, ZDHHC6, and ATP6V0C) that were not identified and 16 proteins with changes deemed not significant in the previous study. The previous study identified 24 EMC-dependent proteins that are not among our list of 36 EMC-dependent proteins, including eight membrane proteins that were not identified in this study, eight soluble proteins, and eight membrane proteins that were identified in our study but their changes were not significant in our analysis. Both studies utilized HeLa cells but differ regarding (1) mutagenesis approaches (CRISPR KO approach versus CRISPRi knockdown), (2) cellular fractions (membrane fractions versus whole-cell lysates), and (3) quantification methods (TMT labeling versus SILAC). These differences may contribute to the variations. In addition, another recent study carried out proteomic analysis on whole-cell lysates of EMC-deficient U2OS cells using SILAC (Volkmar et al., 2019). They reported 11 downregulated proteins, but only two are membrane proteins: FDFT1 and SGPL1. Both were identified in our analysis as well. Together, these studies established a repertoire of EMC-dependent and EMC-independent proteins, providing valuable resources for investigating the mechanism of the EMC.

It is interesting to note that multiple subunits of V-ATPase (ATP6V0A1, ATP6V0C, and TCIRG1) have been identified as EMC-dependent proteins, which might contribute to the effects of loss of the EMC on flavivirus pathogenesis, since these viruses require a low pH within the endosome for membrane fusion. Deviations in endosomal pH levels might also contribute to the reduced sensitivity of EMC-deficient cells to TcdB, as toxin translocation requires low pH levels within endosomes.

Analyzing EMC-dependent proteins revealed that they all contain at least one TMD with polar and/or charged residues. Both our study and the previous proteomic study indicate that the largest portion of EMC clients are denoted as membrane transporters/ion channels, which often contain polar and/or charged residues within their TMDs that are critical for their functions (Shurtleff et al., 2018). It was thus proposed that the function of the EMC is to directly or indirectly integrate TMDs that are energetically unfavorable into the membrane environment (Shurtleff et al., 2018). Here, we took advantage of our validated list of EMC-dependent and EMC-independent membrane proteins and designed mutations within their TMDs, aiming to remove polar and/or charged residues from EMC-dependent proteins or introduce polar residues into EMC-independent proteins. Through trial and error, we converted three EMC-dependent proteins to EMC independent and conversely made two EMC-independent proteins become EMC dependent. These results provide the key experimental evidence supporting that the EMC handles TMDs containing polar and/or charged residues. It is likely that the EMC facilitates the insertion of TMDs as demonstrated for TA proteins and GPCRs (Guna et al., 2018; Chitwood et al., 2018). As our study relies on measuring protein levels rather than the insertion step itself, our data do not exclude the alternative possibility that the EMC may act by protecting the nascent TMDs with polar and/or charged residues from being recognized by quality control machineries as misfolded membrane proteins, thus preventing their subsequent degradation.

EMC-dependent proteins are biased against single-TMD proteins but enriched with more than 4 TMDs, possibly due to a higher chance of containing “hard-to-handle” TMDs within multi-pass membrane proteins. It is also because the TMDs of single-TMD proteins are less likely to perform transporter or other functions that require the presence of polar and/or charged residues. EMC deficiency is tolerated in cultured cells under normal culture conditions, indicating that the membrane integration of challenging TMDs is still possible without the EMC, albeit likely at much reduced efficacy. We note that polar and/or charged residues can also be found in EMC-independent membrane proteins, and the EMC is missing in a few single-cell organisms. Whether there are additional mechanisms to facilitate membrane integration of challenging TMDs remains to be determined. Interestingly, both CFTR and connexin 32 with polar residue mutations in their TMDs become EMC dependent (Coelho et al., 2019; Louie et al., 2012). In fact, many disease-associated membrane protein mutations are the results of introducing polar residues into TMDs (Partridge et al., 2004; Schlebach and Sanders, 2015). Thus, understanding the mechanism by which the EMC handles these challenging TMDs may provide insights and therapeutic targets for treating these genetic disorders.

STAR★METHODS

LEAD CONTACT AND MATERIALS AVAILABILITY

Further information and requests for resources and reagents should be directed to and will be fulfilled by the Lead Contact, Min Dong (min.dong@childrens.harvard.edu). Plasmids generated in this study are freely available upon request to the Lead Contact.

EXPERIMENTAL MODEL AND SUBJECT DETAILS

Cell Lines—HeLa and HEK293T cells were originally purchased from ATCC and propagated in the lab. All the cells were cultured in DMEM media plus 10% fetal bovine serum (FBS) and 100 U penicillin / 0.1 mg/mL streptomycin in a humidified atmosphere of 95% air and 5% CO_2 at 37°C.

METHOD DETAILS

cDNA constructs—ABCD1, ABCB7, SLC27A 4, FDFT1, CD9, SLC43A3, ERGIC3, ATP6V0A1, ZFPL1, SEC61A1 and STT3A with triple-HA or triple-FLAG tag fused to their N terminus (with GSGSGSEF as linker) or C terminus (with EFGSGSGS as linker) were subcloned into pcDNA3.1 vector (Invitrogen, V80020) via Gibson Assembly (NEB, E2621). Mutagenesis was carried out by QuikChange (Agilent, 210519).

Generation of single clone of KO cells and genotyping—The selected sgRNA sequences (EMC4: GCGCTGCTGGGACATCGCCT; EMC6: AGGGCCGCCGTTCATCAGCG) were cloned into LentiGuide-Puro vectors (Addgene, 52963). HeLa-Cas9 was generously provided by Dr. Abraham Brass (Worcester, MA). These Cas9-expressing cells were transduced with lentiviruses that express selected sgRNAs. The mixed stable cell lines were selected using Puromycin (5 μg/mL, ThermoFisher, A1113830). Single clones of KO cells were generated by diluting the mixed KO cells at ~0.8 cell per well in 48-well plates. The genotypes of single cell clones were

determined by amplifying the DNA fragments containing the sgRNA targeting region by PCR, followed by ligating the PCR product into T-vectors (Promega, A3600). The ligation products were transformed into *E. coli* (DH5α strain) and plated onto agar plates. Twenty single colonies were selected, and their plasmids were extracted and sequenced.

Cytopathic assay—The cytopathic effect of $TcdB_{1–1830}$ was analyzed using standard cell-rounding assay as previously described (Tao et al., 2016). Briefly, cells were exposed to a gradient of $TcdB_{1–1830}$ for 24 h. Phase-contrast images of cells were taken (Olympus IX51, 10~20 × objectives). A zone of 300 × 300 μm was selected randomly, which usually contained 50~150 cells. Round-shaped and normal-shaped cells were counted manually. The percentage of round-shaped cells was plotted and fitted using the OriginPro (v8.5) software.

Membrane extraction—Cells were harvested and washed three times with ice-cold PBS. The cell pellets were lysed in PBS (with protease inhibitor cocktail) via sonication. Cell lysates were centrifuged at 500 *g* for 10 min at 4°C. The supernatant was centrifuged at 16,000 *g* for 20 min at 4°C. The pellet was re-suspended in PBS (with protease inhibitor cocktail) and centrifuged at 16,000 *g* for 30 min at 4°C. The pellets were stored in −80°C until analysis.

Immunoblot analysis—Cells were harvested and washed three times with PBS. The cell pellets or membrane fractions were lysed with RIPA buffer (50 mM Tris, pH 7.5, 1% NP40, 150 mM NaCl, 0.5% sodium deoxycholate, 1% SDS, protease inhibitor cocktail). Lysates were centrifuged and the protein amounts in supernatants were measured by BCA assay (ThermoFisher, 23225). The supernatants were heat denatured for 5 min, subjected to SDS-PAGE, and transferred onto a nitrocellulose membrane (GE Healthcare, 10600002). The membrane was blocked with a TBST buffer (10 mM Tris, pH 7.4, 150 mM NaCl, 0.1% Tween-20) containing 5% skim milk at room temperature (RT) for 1 h. Then the membrane was incubated with the primary antibodies for 1 h, then washed and incubated with secondary antibodies for 1 h. The signals were detected using the enhanced chemiluminescence method (ThermoFisher, 34080) by a Fuji LAS3000 imaging system. The relative abundances were quantified by ImageJ.

Quantitative proteomics analysis—Tandem mass tagging (TMT)-based multiplexed quantitative proteomics analysis was carried out as previously described (Qu et al., 2016). Briefly, following protein extraction and concentration measurement by Pierce 660 nm assay, 50 μg protein from each sample was digested by trypsin using the filter-aided sample preparation method, where ammonium bicarbonate was replaced with triethyl ammonium bicarbonate to avoid interference with TMT labeling. Tryptic peptides were labeled with amine-reactive TMT reagents (Thermo Scientific) in parallel, merged into one sample, desalted by C18 spin columns (Thermo Scientific), and concentrated in a SpeedVac (Thermo Scientific). Subsequently, TMT-labeled peptides were reconstituted with 10 mM ammonium formate pH 10.0 and fractionated into 24 fractions by high-pH reversed-phased liquid chromatography using a 10-cm Hypersil GOLD column on an Ultimate 3000 XRS system (Thermo Scientific). The 24 fractions were concatenated into 8 fractions and fractions were sequentially analyzed by low-pH reverse-phase liquid chromatography tandem mass

spectrometry (LC-MS/MS), using a 50-cm EASY-Spray analytical column on an EASY-nLC 1000 system connected to an LTQ Orbitrap Elite mass spectrometer (all from Thermo Scientific). Mass spectra were acquired in a data-dependent manner, selected up to 15 most abundant precursor ions for higher-energy collision dissociation (HCD). To minimize precursor ion co-isolation and to increase reporter ion intensity, the isolation width and normalized collision energy were set at 1.5 m/z and 40, respectively. The acquired raw data were searched against the human UniProt database (released on 01/22/2016, containing 20,985 sequences) with Proteome Discoverer (v2.1), using the SEQUEST algorithm. Search parameters were set as follows: trypsin, up to two missed cleavages; precursor ion tolerance of 10 ppm; fragment ion tolerance of 0.02 Da; carbamidomethylation of cysteines and TMT modification of lysines and peptide N-term as fixed modifications; acetylation of protein N-term and oxidation of methionines as variable modifications. After database search, a stringent 1% false discovery rate (FDR) was set to filter the identifications of peptide-spectrum matches, peptides, and proteins. For protein quantification, peptides with >30% precursor ion interference were excluded. Using Proteome Discoverer, protein ratios were automatically normalized, with the assumption that most proteins were not significantly changed across different samples. Subsequently, Perseus (v1.5.5.3) was applied to identify differentially expressed proteins, using Student's t test followed by Benjaminin-Hochberg FDR correction. Protein level changes were visualized by R program.

Topology analysis—To determine the protein topology, two versions of epitope-tagged proteins into cells via transient transfection, one with HA tag on its N terminus and the other with HA tag on its C terminus. Cells were then permeabilized with two different detergents: Saponin, which permeabilizes both the plasma membrane and the Golgi/ER membrane; or Digitonin, which permeabilizes only the plasma membrane. EMC1 was utilized as control as we previously described (Tian et al., 2018). Cells were transfected with HA-tagged EMC1, ERGIC3, and ERGIC3-Mut1, or co-transfected ERGIC3-Mut1 with EMC4 or EMC6. Cells were washed three times with ice-cold PBS, fixed with 4% paraformaldehyde (PFA) for 20 min at room temperature (RT), permeabilized with either Saponin buffer (0.1% Saponin, 0.1% BSA in PBS) for 30 min at RT or Digitonin buffer (5 μg/mL Digitonin, 0.3 M Sucrose, 0.1 M KCl, 2.5 mM $MgCl_2$, 1 mM EDTA, 10 mM HEPES, pH 6.9) for 15 min at RT. Cells were then blocked with 10% goat serum for 40 min, followed by incubation with anti-HA primary antibodies (1 h) and fluorescence-labeled secondary antibodies (1 h). Slides were sealed within DAPI-containing mounting medium (SouthernBiotech, 0100–20). Fluorescent images were captured with the Olympus DSU-IX81 Spinning Disk Confocal System. Images were pseudo colored and analyzed using ImageJ.

QUANTIFICATION AND STATISTICAL ANALYSIS

Data were considered statistically significant when $p < 0.01$ using Student's t test (double-tail) as indicated in the Figures and Figure legends. Data were represented as mean ± s.d. from three independent biological replicates. Statistical analysis was performed using OriginPro (v8.5) software.

DATA AND CODE AVAILABILITY

The published article includes all dataset generated or analyzed during this study. The full list of quantified 4,446 proteins are included in Data S1.

Supplementary Material

Refer to Web version on PubMed Central for supplementary material.

ACKNOWLEDGMENTS

We thank members of the Dong lab, Dr. A. Kruse (Harvard Medical School), and Dr. T. Rapoport (Harvard Medical School) for discussion. This study was partially supported by grants from NIH (R01NS080833, R01AI132387, R01AI139087, and R21NS106159) and Intelligence Advanced Research Projects Activity (IARPA; W911NF-17-2-0089) to M.D., and by the National Natural Science Foundation of China to Q.W. (81572255). M.D. also acknowledges support from the NIH-funded Harvard Digestive Disease Center (P30DK034854) and Boston Children's Hospital Intellectual and Developmental Disabilities Research Center (P30HD18655). M.D. holds the Investigator in the Pathogenesis of Infectious Disease award from the Burroughs Wellcome Fund.

REFERENCES

Anghel SA, McGilvray PT, Hegde RS, and Keenan RJ (2017). Identification of Oxa1 Homologs Operating in the Eukaryotic Endoplasmic Reticulum. Cell Rep. 21, 3708–3716. [PubMed: 29281821]

Bagchi P, Inoue T, and Tsai B (2016). EMC1-dependent stabilization drives membrane penetration of a partially destabilized non-enveloped virus. eLife 5, e21470. [PubMed: 28012275]

Chitwood PJ, and Hegde RS (2019). The Role of EMC during Membrane Protein Biogenesis. Trends Cell Biol. 29, 371–384. [PubMed: 30826214]

Chitwood PJ, Juszkiewicz S, Guna A, Shao S, and Hegde RS (2018). EMC Is Required to Initiate Accurate Membrane Protein Topogenesis. Cell 175, 1507–1519.e1516. [PubMed: 30415835]

Christianson JC, Olzmann JA, Shaler TA, Sowa ME, Bennett EJ, Richter CM, Tyler RE, Greenblatt EJ, Harper JW, and Kopito RR (2011). Defining human ERAD networks through an integrative mapping strategy. Nat. Cell Biol 14, 93–105. [PubMed: 22119785]

Coelho JPL, Stahl M, Bloemeke N, Meighen-Berger K, Alvira CP, Zhang ZR, Sieber SA, and Feige MJ (2019). A network of chaperones prevents and detects failures in membrane protein lipid bilayer integration. Nat. Commun 10, 672. [PubMed: 30737405]

Denic V, Dötsch V, and Sinning I (2013). Endoplasmic reticulum targeting and insertion of tail-anchored membrane proteins by the GET pathway. Cold Spring Harb. Perspect. Biol 5, a013334. [PubMed: 23906715]

Guna A, Volkmar N, Christianson JC, and Hegde RS (2018). The ER membrane protein complex is a transmembrane domain insertase. Science 359, 470–73. [PubMed: 29242231]

Harel T, Yesil G, Bayram Y, Coban-Akdemir Z, Charng WL, Karaca E, Al Asmari A, Eldomery MK, Hunter JV, Jhangiani SN, et al.; Baylor-Hopkins Center for Mendelian Genomics (2016). Monoallelic and Biallelic Variants in EMC1 Identified in Individuals with Global Developmental Delay, Hypotonia, Scoliosis, and Cerebellar Atrophy. Am. J. Hum. Genet 98, 562–570. [PubMed: 26942288]

Hegde RS, and Keenan RJ (2011). Tail-anchored membrane protein insertion into the endoplasmic reticulum. Nat. Rev. Mol. Cell Biol 12, 787–798. [PubMed: 22086371]

Jonikas MC, Collins SR, Denic V, Oh E, Quan EM, Schmid V, Weibezahn J, Schwappach B, Walter P, Weissman JS, and Schuldiner M (2009). Comprehensive characterization of genes required for protein folding in the endoplasmic reticulum. Science 323, 1693–1697. [PubMed: 19325107]

Lahiri S, Chao JT, Tavassoli S, Wong AK, Choudhary V, Young BP, Loewen CJ, and Prinz WA (2014). A conserved endoplasmic reticulum membrane protein complex (EMC) facilitates phospholipid transfer from the ER to mitochondria. PLoS Biol. 12, e1001969. [PubMed: 25313861]

Li Y, Zhao Y, Hu J, Xiao J, Qu L, Wang Z, Ma D, and Chen Y (2013). A novel ER-localized transmembrane protein, EMC6, interacts with RAB5A and regulates cell autophagy. Autophagy 9, 150–163. [PubMed: 23182941]

Lin DL, Inoue T, Chen YJ, Chang A, Tsai B, and Tai AW (2019). The ER Membrane Protein Complex Promotes Biogenesis of Dengue and Zika Virus Non-structural Multi-pass Transmembrane Proteins to Support Infection. Cell Rep. 27, 1666–1674.e1664. [PubMed: 31067454]

Louie RJ, Guo J, Rodgers JW, White R, Shah N, Pagant S, Kim P, Livstone M, Dolinski K, McKinney BA, et al. (2012). A yeast phenomic model for the gene interaction network modulating CFTR-ΔF508 protein biogenesis. Genome Med. 4, 103. [PubMed: 23270647]

Ma H, Dang Y, Wu Y, Jia G, Anaya E, Zhang J, Abraham S, Choi JG, Shi G, Qi L, et al. (2015). A CRISPR-Based Screen Identifies Genes Essential for West-Nile-Virus-Induced Cell Death. Cell Rep. 12, 673–683. [PubMed: 26190106]

Marceau CD, Puschnik AS, Majzoub K, Ooi YS, Brewer SM, Fuchs G, Swaminathan K, Mata MA, Elias JE, Sarnow P, and Carette JE (2016). Genetic dissection of Flaviviridae host factors through genome-scale CRISPR screens. Nature 535, 159–163. [PubMed: 27383987]

Partridge AW, Therien AG, and Deber CM (2004). Missense mutations in transmembrane domains of proteins: phenotypic propensity of polar residues for human disease. Proteins 54, 648–656. [PubMed: 14997561]

Qu Y, Zhou B, Yang W, Han B, Yu-Rice Y, Gao B, Johnson J, Svendsen CN, Freeman MR, Giuliano AE, et al. (2016). Transcriptome and proteome characterization of surface ectoderm cells differentiated from human iPSCs. Sci. Rep 6, 32007. [PubMed: 27550649]

Rapoport TA, Li L, and Park E (2017). Structural and Mechanistic Insights into Protein Translocation. Annu. Rev. Cell Dev. Biol 33, 369–390. [PubMed: 28564553]

Richard M, Boulin T, Robert VJ, Richmond JE, and Bessereau JL (2013). Biosynthesis of ionotropic acetylcholine receptors requires the evolutionary conserved ER membrane complex. Proc. Natl. Acad. Sci. USA 110, E1055–E1063. [PubMed: 23431131]

Satoh T, Ohba A, Liu Z, Inagaki T, and Satoh AK (2015). dPob/EMC is essential for biosynthesis of rhodopsin and other multi-pass membrane proteins in Drosophila photoreceptors. eLife 4, 4.

Savidis G, McDougall WM, Meraner P, Perreira JM, Portmann JM, Trincucci G, John SP, Aker AM, Renzette N, Robbins DR, et al. (2016). Identification of Zika Virus and Dengue Virus Dependency Factors using Functional Genomics. Cell Rep. 16, 232–246. [PubMed: 27342126]

Schlebach JP, and Sanders CR (2015). Influence of Pathogenic Mutations on the Energetics of Translocon-Mediated Bilayer Integration of Transmembrane Helices. J. Membr. Biol 248, 371–381. [PubMed: 25192979]

Shao S, and Hegde RS (2011). Membrane protein insertion at the endoplasmic reticulum. Annu. Rev. Cell Dev. Biol 27, 25–56. [PubMed: 21801011]

Shen X, Kan S, Hu J, Li M, Lu G, Zhang M, Zhang S, Hou Y, Chen Y, and Bai Y (2016). EMC6/TMEM93 suppresses glioblastoma proliferation by modulating autophagy. Cell Death Dis. 7, e2043. [PubMed: 26775697]

Shurtleff MJ, Itzhak DN, Hussmann JA, Schirle Oakdale NT, Costa EA, Jonikas M, Weibezahn J, Popova KD, Jan CH, Sinitcyn P, et al. (2018). The ER membrane protein complex interacts cotranslationally to enable biogenesis of multipass membrane proteins. eLife 7, e37018. [PubMed: 29809151]

Tang X, Snowball JM, Xu Y, Na CL, Weaver TE, Clair G, Kyle JE, Zink EM, Ansong C, Wei W, et al. (2017). EMC3 coordinates surfactant protein and lipid homeostasis required for respiration. J. Clin. Invest 127, 4314–4325. [PubMed: 29083321]

Tao L, Zhang J, Meraner P, Tovaglieri A, Wu X, Gerhard R, Zhang X, Stallcup WB, Miao J, He X, et al. (2016). Frizzled proteins are colonic epithelial receptors for C. difficile toxin B. Nature 538, 350–355. [PubMed: 27680706]

Tian S, Muneeruddin K, Choi MY, Tao L, Bhuiyan RH, Ohmi Y, Furukawa K, Furukawa K, Boland S, Shaffer SA, et al. (2018). Genome-wide CRISPR screens for Shiga toxins and ricin reveal Golgi proteins critical for glycosylation. PLoS Biol. 16, e2006951. [PubMed: 30481169]

Volkmar N, Thezenas ML, Louie SM, Juszkiewicz S, Nomura DK, Hegde RS, Kessler BM, and Christianson JC (2019). The ER membrane protein complex promotes biogenesis of sterol-related enzymes maintaining cholesterol homeostasis. J. Cell Sci. 132, jcs223453. [PubMed: 30578317]

Wideman JG (2015). The ubiquitous and ancient ER membrane protein complex (EMC): tether or not? F1000Res. 4, 624. [PubMed: 26512320]

Zhang R, Miner JJ, Gorman MJ, Rausch K, Ramage H, White JP, Zuiani A, Zhang P, Fernandez E, Zhang Q, et al. (2016). A CRISPR screen defines a signal peptide processing pathway required by flaviviruses. Nature 535, 164–168. [PubMed: 27383988]

Highlights

- Proteomic analysis of membrane protein expression levels in EMC-deficient cells
- 36 EMC-dependent and 171 EMC-independent membrane proteins were established
- EMC-dependent proteins contain polar and/or charged residues in transmembrane domains
- EMC dependency can be converted by removing or introducing polar and/or charged residues

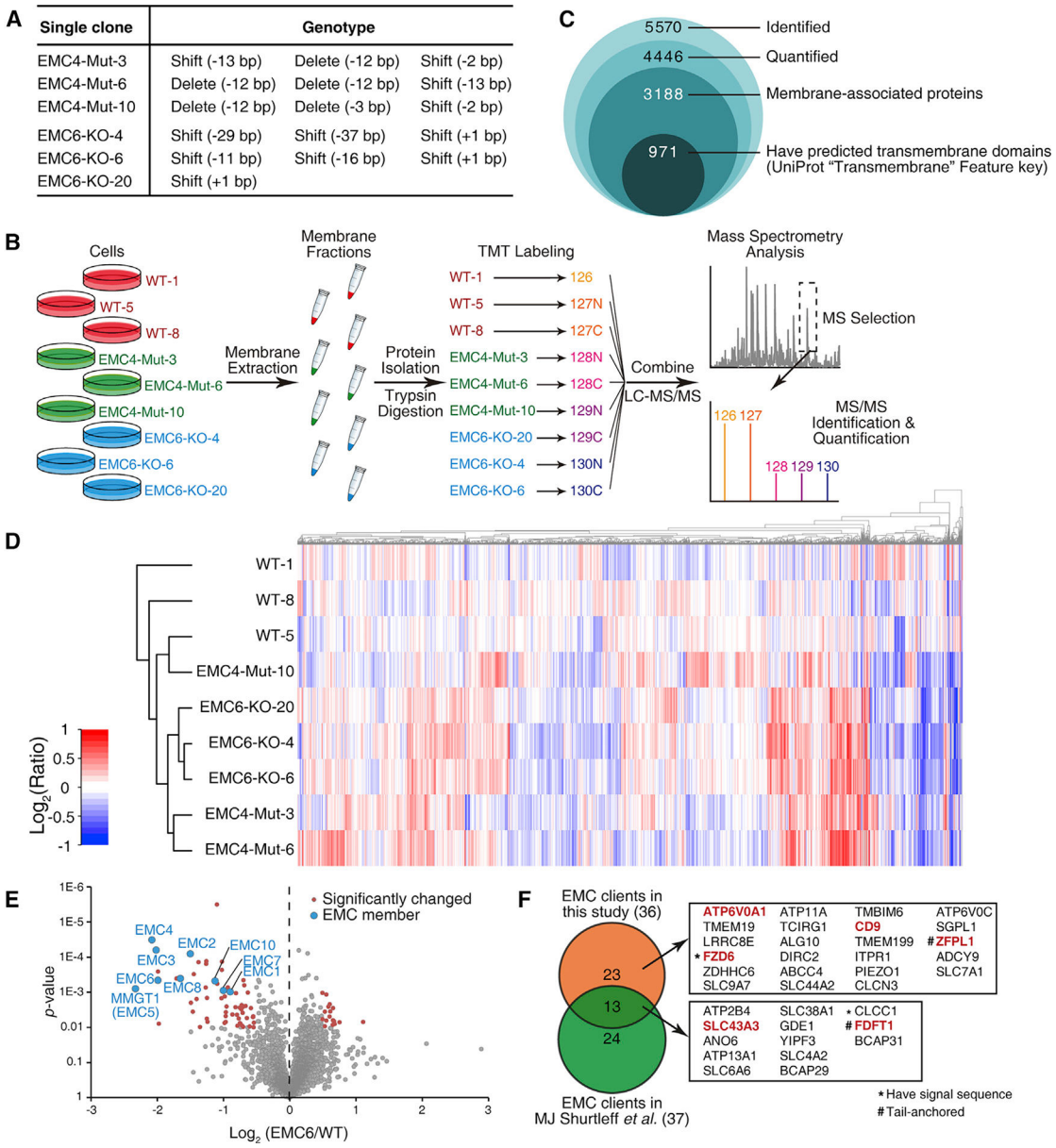

Figure 1. Quantitative Proteomics Analysis of EMC-Deficient Cell Lines

(A) Genotypes of EMC-deficient cell lines. Shift, frameshift mutation; Delete, deletion mutation; bp, base pair.

(B) Schematic diagram of the quantitative proteomics analysis process.

(C) Summary of the proteins identified.

(D) Heat-map and clustering analysis using Pearson distance of 4,446 proteins quantified in our proteomic analysis. The color key shows the $\log_2$ transformed protein amount ratios.

(E) Volcano plot of fold-change and statistical significance of all 4,446 proteins quantified. The protein levels in EMC6-KO cells over WT cells were plotted as the x axis (shown as $\log_2$ value of their ratio). The statistical significance (p value, Student's t test) was plotted as the y axis.

(F) Venn diagram showing the overlap between EMC-dependent proteins identified in this study and those previously reported by Shurtleff et al. (2018). The 13 overlapping proteins and the 23 proteins unique to this study are listed. Red color marks the ones validated in this study; asterisks mark the ones with signal sequences; # marks tail-anchored proteins.

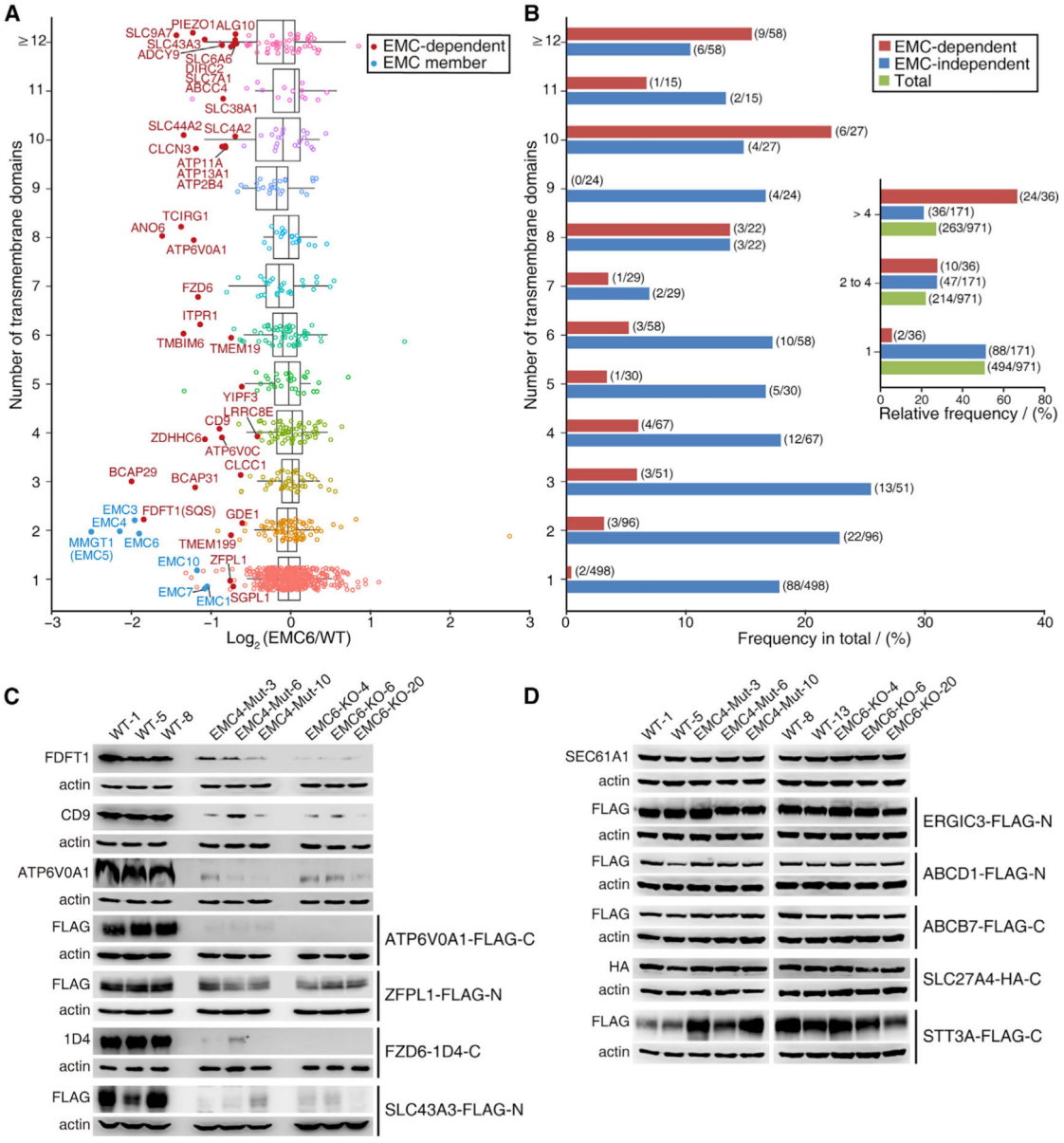

Figure 2. EMC-Dependent Proteins Contain Various Numbers of TMDs

(A) All 971 membrane proteins with UniProt "Transmembrane" feature key were categorized based on the number of their TMDs. The x axis shows the $\log_2$ ratios of protein levels in EMC6-KO over WT cells, and the y axis shows the number of TMDs. EMC-dependent proteins (red dots) and EMC members (blue dots) are highlighted. The proteins with more than 11 TMDs were clustered as one group (≥12).

(B) The number of identified EMC-dependent proteins (red bars) and EMC-independent proteins (blue bars) over the total number of transmembrane proteins with the same number of TMDs within 971 transmembrane proteins. The inside panel shows the relative frequency for three groups: single TMD, 2–4 TMDs, and more than 4 TMDs among identified 36 EMC-dependent, 171 EMC-independent, and all 971 transmembrane proteins, respectively.

(C) Validation of EMC-dependent proteins. Expression levels of FDFT1, CD9, and ATP6V0A1 in WT, EMC4-Mut, and EMC6-KO cells were analyzed by immunoblot using antibodies targeting endogenous proteins. ATP6V0A1, ZFPL1, FZD6, and SLC43A3 with the indicated fusion tags were expressed in WT cell lines and EMC-deficient cell lines via transient transfection. Actin served as a loading control. FLAG-N, N-terminal triple-FLAG tag; FLAG-C, C-terminal triple-FLAG tag; 1D4-C, C-terminal 1D4 tag.

(D) Validation of EMC-independent proteins. Endogenous SEC61A1 in WT cell lines and EMC-deficient cell lines were detected via immunoblot using an anti-SEC61A1 antibody, while other indicated EMC-independent proteins were expressed in WT and EMC-deficient cell lines via transient transfection and detected via fused FLAG or HA tags by immunoblot analysis. HA-C, C-terminal triple-HA tag.

In (C) and (D), representative images were from one of three independent experiments.

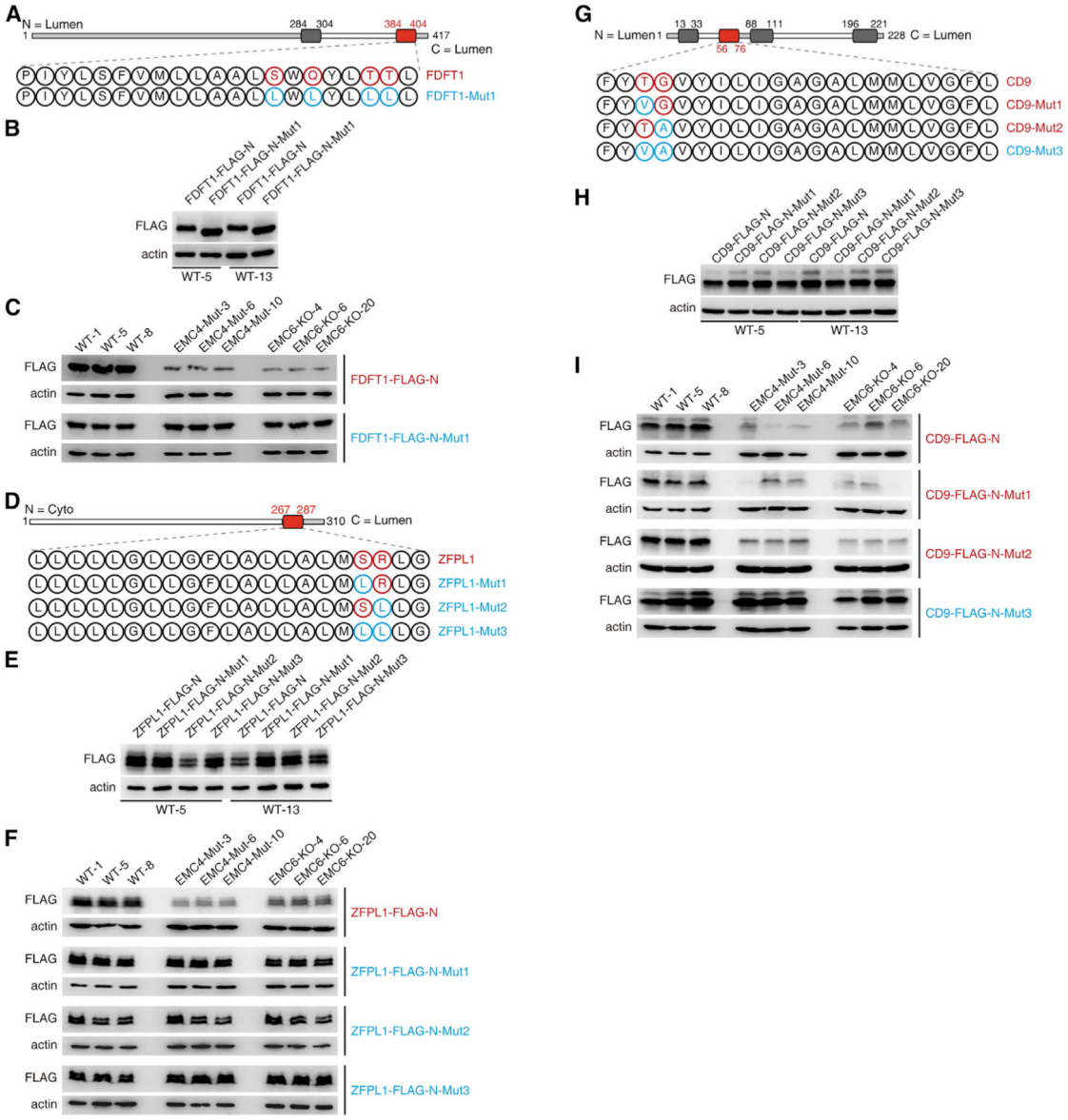

Figure 3. Removing Polar and/or Charged Residues within TMDs Changes EMC-Dependent Proteins to Become EMC Independent

(A) The residues in the second TMD (marked in red) of WT and the indicated FDFT1 mutant are shown.

(B) WT and the indicated FDFT1 mutant were expressed at similar levels in two WT cell lines (WT-5 and WT-13) via transient transfection. Actin served as a loading control.

(C) WT and the FDFT1 mutant were expressed in WT and EMC-deficient cell lines via transient transfection, and their expression levels were analyzed by immunoblot.

(D) ZFPL1 is a single-TMD protein, with WT and mutant residues within its TMD marked.

(E) WT and the indicated ZFPL1 mutants were expressed at similar levels in WT cell lines via transient transfection.

(F) WT and the indicated ZFPL1 mutants were expressed in WT and EMC-deficient cells via transient transfection, and their expressions were examined via immunoblot.

(G) CD9 contains 4 TMDs, with both WT and mutant residues within its second TMD (marked in red) shown.
(H) WT and the indicated CD9 mutants were expressed at similar levels when transfected into WT cell lines.
(I) WT and the indicated CD9 mutants were expressed in WT and EMC-deficient cells via transient transfection. Their expression levels were examined via immunoblot.
In (B), (C), (E), (F), (H), and (I), representative images were from one of three independent experiments.

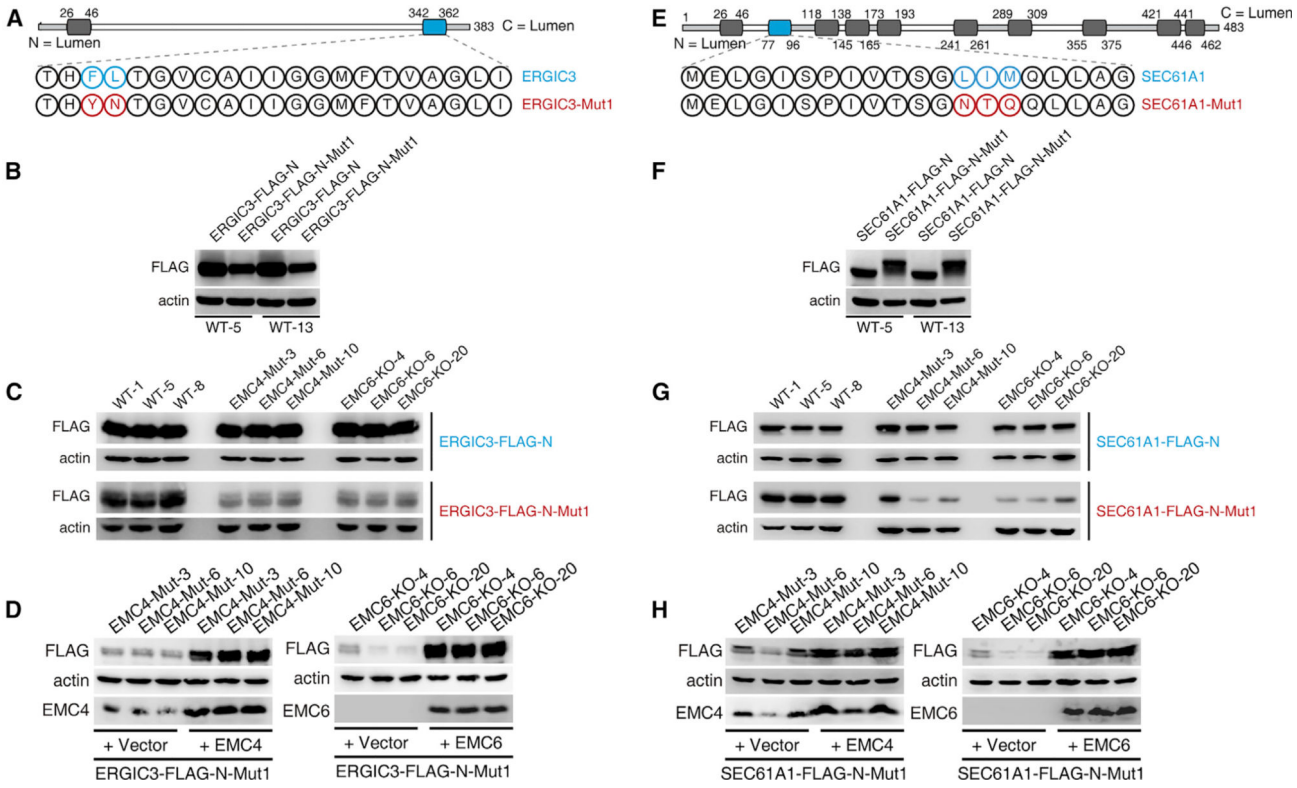

Figure 4. Introducing Polar Residues to TMDs Converts EMC-Independent Proteins to EMC-Dependent Proteins

(A) ERGIC3 contains 2 TMDs, with WT and the mutated residues within its second TMD (marked as blue) listed.

(B) WT and the indicated ERGIC3 mutant showed similar levels of expression in WT cells. Actin served as a loading control.

(C) WT and the indicated ERGIC3 mutant were expressed in WT and EMC-deficient cells via transient transfection. Their expression levels were examined via immunoblot.

(D) Expression of EMC4 in EMC4-Mut cells and EMC6 in EMC6-KO cells elevated expression levels of co-transfected ERGIC3-FLAG-N-Mut1 in these EMC-deficient cells.

(E) SEC61A1 is a 10-TMD protein, with WT and the mutated residues within its second TMD (marked as blue) listed.

(F) WT and the indicated SEC61A1 mutant are expressed at similar levels in WT cells.

(G) WT and the indicated SEC61A1 mutant were expressed in WT and EMC-deficient cells via transient transfection. Their expressions were examined via immunoblot.

(H) Expression of EMC4 in EMC4-Mut cells and EMC6 in EMC6-KO cells elevated expression levels of co-transfected SEC61A1-FLAG-N-Mut1 in these EMC-deficient cells.

In (B), (C), (D), (F), (G), and (H), representative images were from one of three independent experiments.

KEY RESOURCES TABLE

REAGENT or RESOURCE	SOURCE	IDENTIFIER
Antibodies		
Mouse monoclonal anti-Actin	Aves Labs	ACT-1010
Rabbit monoclonal anti-FDFT1	Abcam	ab195046
Rabbit monoclonal anti-CD9	Abcam	ab92726
Rabbit polyclonal anti-ATP6V0A1	Abcam	ab176858
Mouse monoclonal anti-HA	BioLegend	901502
Mouse monoclonal anti-FLAG	Sigma	F3165
Mouse monoclonal anti-Rhodopsin (1D4)	ThermoFisher	MA1–722
Rabbit monoclonal anti-EMC4	Abcam	ab184544
Rabbit polyclonal anti-EMC6	Abcam	ab84902
Mouse monoclonal anti-SYT1	Synaptic System	105011
Rabbit monoclonal anti-SEC61A1	Abcam	ab183046
Rabbit monoclonal anti-BiP	Cell Signaling	C50B12
Chemicals, Peptides, and Recombinant Proteins		
PolyJet	SignaGen	SL100688
MG-132	Sigma	M8699
Lactacystin	Sigma	L6785
$TcdB_{1–1830}$	Liang Tao	Reference (Tao et al., 2016)
Dulbecco's Modified Eagle Medium	Life technologies	Cat#11995–065
Fetal bovine serum	Life technologies	Cat#26140–079
Penicillin/streptomycin	Life technologies	Cat#15140–122
Puromycin	ThermoFisher	A1113830
T-vectors	Promega	A3600
Protease Inhibitor Cocktail	Roche	4693159001
Nitrocellulose membrane	GE Healthcare	10600002
Chemiluminescent Substrate	ThermoFisher	34080
Digitonin	Sigma	D141
Saponin	Sigma	84510
DAPI-containing mounting medium	SouthernBiotech	0100–20
Critical Commercial Assays		
Gibson Assembly	NEB	E2621
QuikChange kit	Agilent	210519
BCA assay kit	ThermoFisher	23225
TMT reagents	ThermoFisher	A34808
Experimental Models: Cell Lines		
HeLa	ATCC	CCL-2
HeLa-Cas9	Abraham Brass	N/A

REAGENT or RESOURCE	SOURCE	IDENTIFIER
HEK293T	ATCC	CRL-3216
WT-1	This paper	N/A
WT-5	This paper	N/A
WT-8	This paper	N/A
WT-13	This paper	N/A
EMC4-Mut-3	This paper	N/A
EMC4-Mut-6	This paper	N/A
EMC4-Mut-10	This paper	N/A
EMC6-KO-4	This paper	N/A
EMC6-KO-6	This paper	N/A
EMC6-KO-20	This paper	N/A
Oligonucleotides		
See Table S1 for oligonucleotides used in these studies	This paper	N/A
Recombinant DNA		
ABCD1cDNA	GE Dharmacon	3896490
ABCB7 cDNA	GE Dharmacon	4138236
SLC27A4 cDNA	GE Dharmacon	6023438
FDFT1 cDNA	GE Dharmacon	4514761
CD9 cDNA	GE Dharmacon	3860667
SLC43A3 cDNA	GE Dharmacon	2958307
ERGIC3 cDNA	OriGene	SC319922
ATP6V0A1 cDNA	OriGene	SC116892
ZFPL1 cDNA	Sino Biology	HG25532-U
SEC61A1 cDNA	Sino Biology	HG19659-NY
EMC1cDNA	GE Dharmacon	4831005
EMC4 cDNA	GenScript	OHu00964
EMC6 cDNA	GenScript	OHu00989
STT3A pEGFP-N2	Addgene	62025
pRK5-mFzd1–1D4	Addgene	42263
pRK5-mFzd2–1D4	Addgene	42264
pRK5-mFzd4–1D4	Addgene	42266
pRK5-mFzd6–1D4	Addgene	42268
pRK5-mFzd7–1D4	Addgene	42269
pcDNA3.1	ThermoFisher	V80020
pMD2.G	Addgene	#12259
pSPAX2	Addgene	#12260
LentiGuide-puro	Addgene	#52963
lenti-SpCas9 blast	Addgene	#104997
pEGFP-N1	Clonetech	#6085–1

REAGENT or RESOURCE	SOURCE	IDENTIFIER
pcDNA-SytI	Min Dong	N/A
LentiGuide-EMC4	This paper	N/A
LentiGuide-EMC6	This paper	N/A
pcDNA3.1-EMC4-sgRNA resistent	This paper	N/A
pcDNA3.1-EMC6-sgRNA resistent	This paper	N/A
pcDNA3.1-FDFT1-FLAG-N	This paper	N/A
pcDNA3.1-FDFT1-FLAG-N-Mut1	This paper	N/A
pcDNA3.1-CD9-FLAG-N	This paper	N/A
pcDNA3.1-CD9-FLAG-N-Mut1	This paper	N/A
pcDNA3.1-CD9-FLAG-N-Mut2	This paper	N/A
pcDNA3.1-CD9-FLAG-N-Mut3	This paper	N/A
pcDNA3.1-ATP6V0A1-FLAG-C	This paper	N/A
pcDNA3.1-ZFPL1-FLAG-N	This paper	N/A
pcDNA3.1-ZFPL1-FLAG-N-Mut1	This paper	N/A
pcDNA3.1-ZFPL1-FLAG-N-Mut2	This paper	N/A
pcDNA3.1-ZFPL1-FLAG-N-Mut3	This paper	N/A
pcDNA3.1-SLC43A3-FLAG-N	This paper	N/A
pcDNA3.1-ERGIC3-FLAG-N	This paper	N/A
pcDNA3.1-ERGIC3-FLAG-N-Mut1	This paper	N/A
pcDNA3.1-ABCD1 -FLAG-N	This paper	N/A
pcDNA3.1-ABCB7-FLAG-C	This paper	N/A
pcDNA3.1-SLC27A4-HA-C	This paper	N/A
pcDNA3.1-STT3A-FLAG-C	This paper	N/A
pcDNA3.1-SEC61A1-FLAG-N	This paper	N/A
pcDNA3.1-SEC61A1-FLAG-N-Mut1	This paper	N/A
pcDNA3.1-EMC1-HA-N	This paper	N/A
pcDNA3.1-EMC1-HA-C	This paper	N/A
pcDNA3.1-ERGIC3-HA-N	This paper	N/A
pcDNA3.1-ERGIC3-HA-C	This paper	N/A
pcDNA3.1-ERGIC3-HA-N-Mut1	This paper	N/A
pcDNA3.1-ERGIC3-HA-C-Mut1	This paper	N/A
pcDNA3.1-FDFT1-FLAG-C	This paper	N/A
Software and Algorithms		
OriginPro	OriginLab	v8.5
Excel	Microsoft	2007
ImageJ	https://imagej.nih.gov/ij/	Version 1.52o
Proteome Discoverer	ThermoFisher	v2.1

REAGENT or RESOURCE	SOURCE	IDENTIFIER
Perseus	https://www.maxquant.net/perseus/	v1.5.5.3
R program	https://www.r-project.org/	v3.3.3